



4-[(Benzylamino)carbonyl]-1-methylpyridinium bromide hemihydrate: X-ray diffraction study and Hirshfeld surface analysis

Vitalii V. Rudiuk,^{a,b} Anna M. Shaposhnik,^c Vyacheslav M. Baumer,^c Igor A. Levandovskiy^b and Svitlana V. Shishkina^{c,d*}

Received 14 October 2021

Accepted 6 April 2022

Edited by M. Weil, Vienna University of Technology, Austria

Keywords: 4-[(benzylamino)carbonyl]-1-methylpyridinium bromide; molecular structure; crystal structure; Hirshfeld surface analysis.

CCDC reference: 2164796

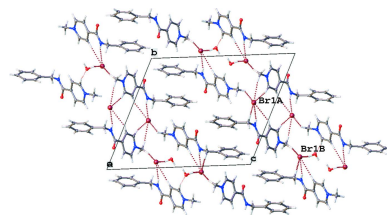
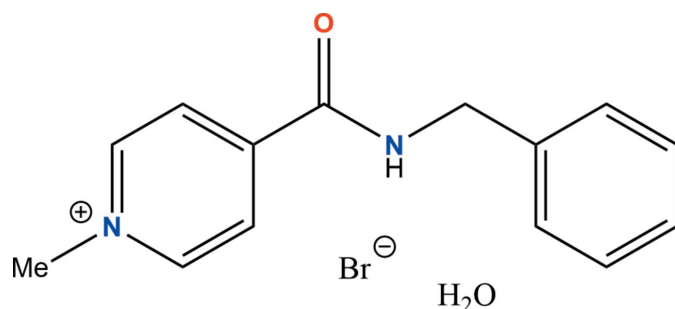
Supporting information: this article has supporting information at journals.iucr.org/e

^aFarmak JSC, 63 Kyrylivska str., Kyiv 04080, Ukraine, ^bDepartment of Organic Chemistry, National Technical University of Ukraine, 37, Pobedy ave., Kyiv, 03056, Ukraine, ^cSSI "Institute for Single Crystals" NAS of Ukraine, 60 Nauky ave., Kharkiv, 61001, Ukraine, and ^dV.N. Karazin Kharkiv National University, 4 Svobody sq., Kharkiv 61022, Ukraine.
*Correspondence e-mail: sveta@xray.isc.kharkov.com

The hemihydrate of 4-[(benzylamino)carbonyl]-1-methylpyridinium bromide, $C_{14}H_{15}N_2O^+\cdot Br^- \cdot 0.5H_2O$, was studied by single-crystal and powder X-ray diffraction methods. In the asymmetric unit, two organic cations of similar conformation, two bromide anions and one water molecule are present. In the crystal, $N-H \cdots Br$ hydrogen bonds link the cations and anions. The formation of a set of intermolecular $C-H \cdots Br$ and $C-H \cdots \pi$ interactions result in double chains extending parallel to [011]. A Hirshfeld surface analysis showed high contributions of $H \cdots H$ and $C \cdots H/H \cdots C$ short contacts to the total Hirshfeld surfaces of the cations.

1. Chemical context

The 4-[(benzylamino)carbonyl]-1-methylpyridinium cation (Am^+) has been shown to possess antiviral activity (Buhtiarova *et al.*, 2003; Frolov *et al.*, 2004; Boltz *et al.*, 2018; te Velthuis *et al.*, 2021). Being charged due to quaternization of the pyridine N atom, this type of cation is more stable than its protonated analogue formed by H-atom transition in the form of an acid–base pair. Halogenide anions can be used as simple counter-ions of the organic cation. In fact, the iodide salt of 4-[(benzylamino)carbonyl]-1-methylpyridinium (AmI) is known as a multimodal antiviral drug and has been studied by single-crystal X-ray diffraction, powder diffraction, IR spectroscopy, and DSC methods (Drebushchak *et al.*, 2017). The search for polymorphic modifications, hydrates or solvates is of great importance for the pharmaceutical industry to improve the quality of a drug and to protect intellectual property. However, polymorphic screening performed for the AmI salt did not reveal any other crystalline form.



OPEN ACCESS

Published under a CC BY 4.0 licence

Table 1

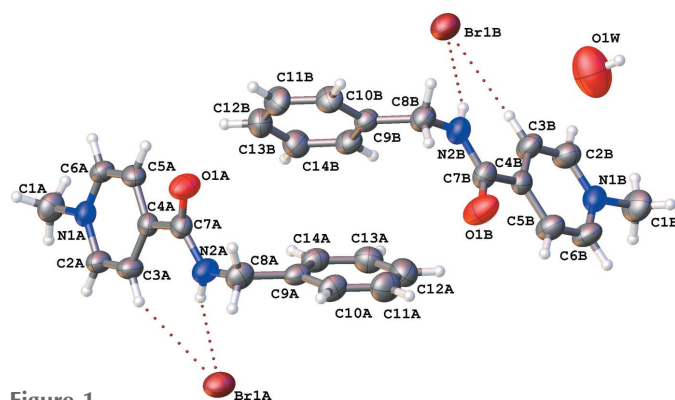
Some geometrical characteristics (\AA , $^\circ$) of cations *A* and *B* in AmBr hemihydrate.

Parameter	Cation <i>A</i>	Cation <i>B</i>
N1—C2	1.343 (6)	1.323 (7)
N1—C6	1.330 (7)	1.329 (7)
N2—C7—C4—C3	17.1 (7)	-1.4 (9)
C7—N2—C8—C9	-102.6 (6)	-107.0 (6)
N2—C8—C9—C10	-168.9 (5)	-167.4 (5)
H2···H3	2.11	2.04
H2···C3	2.59	2.54

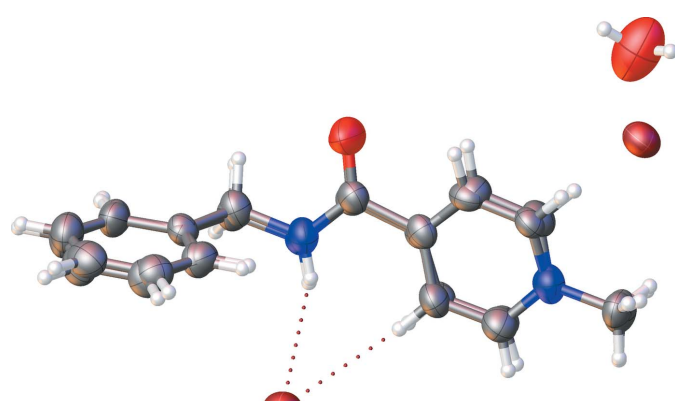
The 4-[(benzylamino)carbonyl]-1-methylpyridinium bromide (AmBr) salt is the closest analogue of AmI. Polymorphic screening for this salt resulted in the crystallization of a hemihydrate. In this communication we present the molecular and crystal structures of 4-[(benzylamino)carbonyl]-1-methylpyridinium bromide hemihydrate, $(\text{C}_{14}\text{H}_{15}\text{N}_2\text{O})^+\text{Br}^- \cdot 0.5\text{H}_2\text{O}$.

2. Structural commentary

The asymmetric unit contains two molecules of the cation (denoted *A* and *B*), two bromide anions (*A* and *B*) and one water molecule (Fig. 1). The positive charge of the cation is located at the quaternized nitrogen atom of the pyridine ring.

**Figure 1**

Molecular structure of the title compound, AmBr hemihydrate. Displacement ellipsoids are shown at the 50% probability level. C—H···Br and N—H···Br hydrogen bonds are indicated by dotted lines.

**Figure 2**

Molecular overlay plot of cations *A* and *B*.

Table 2

Hydrogen-bond geometry (\AA , $^\circ$).

CgA and CgB are the centroids of the C9A–C14A and C9B–C14B rings, respectively.

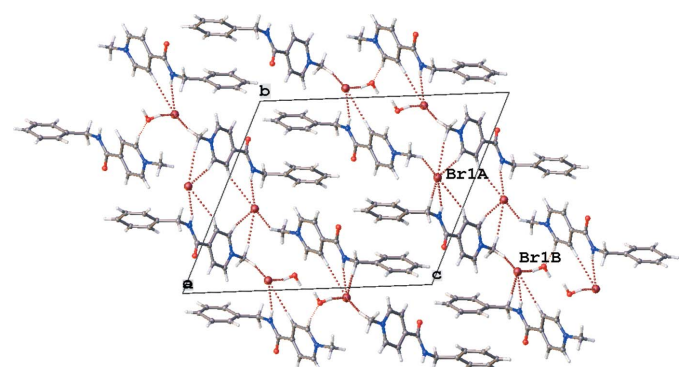
$D-\text{H}\cdots A$	$D-\text{H}$	$\text{H}\cdots A$	$D\cdots A$	$D-\text{H}\cdots A$
N2A—H2A···Br1A	0.86	2.53	3.339 (5)	158
C3A—H3A···Br1A	0.93	2.98	3.814 (5)	150
C2A—H2AA···Br1A ⁱ	0.93	2.84	3.725 (6)	159
C1A—H1AA···Br1A ⁱ	0.96	2.88	3.784 (6)	157
C6A—H6A··· CgB^{ii}	0.93	2.65	3.510 (7)	154
N2B—H2B···Br1B	0.86	2.60	3.419 (5)	159
C3B—H3B···Br1B	0.93	2.83	3.753 (5)	175
C6B—H6B··· CgB^{iii}	0.93	2.71	3.400 (7)	132
O1W—H1WA···Br1B ^{iv}	0.85	3.03	3.473 (7)	115
C1A—H1AC···O1W ^v	0.96	2.89	3.794 (10)	157

Symmetry codes: (i) $-x+2, -y+2, -z+2$; (ii) $-x+1, -y+1, -z+2$; (iii) $-x+1, -y+2, -z+1$; (iv) $-x+1, -y+1, -z+1$; (v) $x+1, y, z+1$.

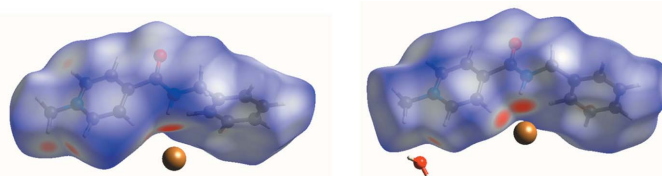
The carbamide group is slightly non-coplanar with the plane of the aromatic ring, as shown by the N2—C7—C4—C3 torsion angles given in Table 1. The non-planarity is caused by steric repulsion between the two constituents as revealed by the amide H2···H3_{pyridine} and amide H2···C3_{pyridine} short contacts (Table 1) as compared to the van der Waals radii sums (Zefirov, 1997) of 2.34 and 2.87 \AA , respectively. The cations *A* and *B* have similar conformations of the benzyl substituent (Fig. 2). The phenyl fragment of the benzyl substituent is located in an *ac* position in relation to the C7—N2 bond and is twisted in relation to the carbamide fragment in both cations *A* and *B*, as seen in the C7—N2—C8—C9 and N2—C8—C9—C10 torsion angles (Table 1).

3. Supramolecular features

In the crystal, cations *A* and *B* interact with the bromide anions by N—H···Br hydrogen bonds. In addition, a set of C—H···Br and C—H··· π interactions are found in the crystal structure (Table 2). The solvent water molecule forms one C—H···O hydrogen bond as a proton acceptor and O—H···Br and O—H···O hydrogen bonds as a proton donor (Table 2). All these hydrogen-bonding interactions result in the formation of double chains extending parallel to [011] (Fig. 3).

**Figure 3**

Crystal packing of AmBr hemihydrate in a view along [100]. Hydrogen-bonding interactions are shown by dashed lines.

**Figure 4**

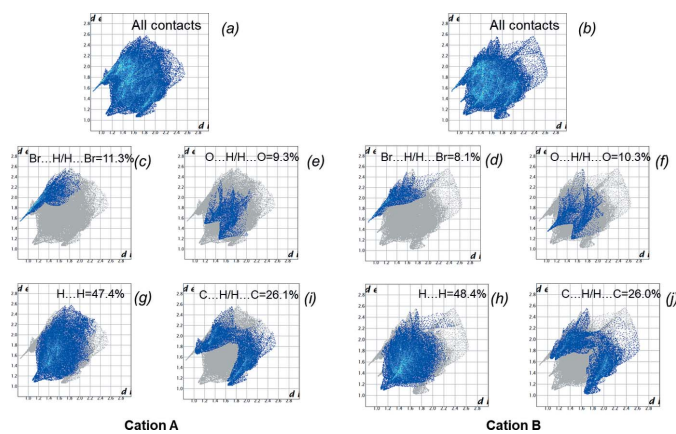
Hirshfeld surfaces mapped over d_{norm} for cations *A* (left) and *B* (right) in the crystal structure of AmBr hemihydrate.

4. Hirshfeld surface analysis

Intermolecular interactions were analysed using Hirshfeld surface analysis and two-dimensional fingerprint plots by using *CrystalExplorer17* (Turner *et al.*, 2017). The Hirshfeld surfaces were calculated separately for cations *A* and *B* using a standard high surface resolution, mapped over d_{norm} (Fig. 4). The red spots corresponding to contacts that are shorter than the van der Waals radii sum of the closest atoms are observed at the hydrogen atom of the amino group and at some phenyl and methyl hydrogen atoms. The two-dimensional fingerprint plots showed the absence of strong hydrogen bonds in the structure under study. To compare intermolecular interactions of different types in a more quantitative way, their contributions to the total Hirshfeld surfaces were analysed (Fig. 5). The main contribution is provided by H···H short contacts (Fig. 5*g,h*). The contribution of C···H/H···C short contacts is also significant (Fig. 5*i,j*). The Br···H/H···Br and O···H/H···O interactions contribute to the total Hirshfeld surface in the same way (Fig. 5*c,d* and 5*e,f*).

5. Database survey

A search of the Cambridge Structural Database (Version 5.42, update of November 2020; Groom *et al.*, 2016) revealed the structure of the anhydrous AmI salt with an equimolar cation:iodine ratio (refcode BEBFIA; Drebushchak *et al.*, 2017). A comparison of the molecular conformation of the cation showed its flexibility due to rotation about the N—C_{sp}³ and C_{sp}³—C_{aryl} bonds.

**Figure 5**

Contributions of interactions of different types to the total Hirshfeld surface of cations *A* and *B* in the crystal structure of AmBr hemihydrate.

Table 3

Experimental data of the X-ray powder diffraction study performed at 293 K.

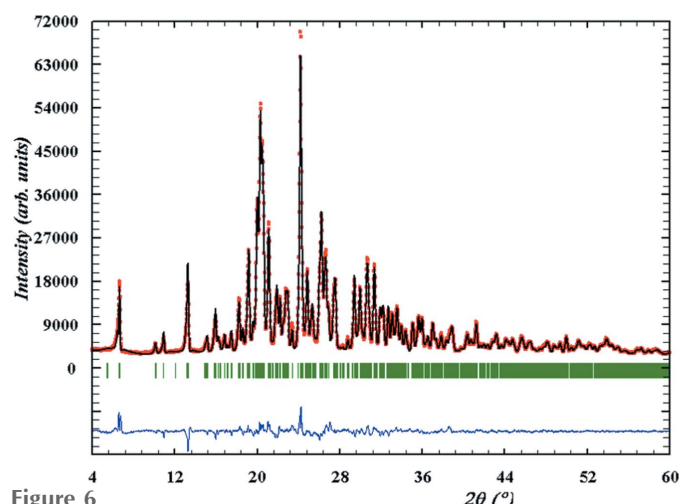
Crystal system, space group	Triclinic, <i>P</i> 1
<i>a</i> (Å)	5.8858 (2)
<i>b</i> (Å)	14.7604 (3)
<i>c</i> (Å)	17.8118 (4)
α (°)	65.819 (1)
β (°)	85.321 (2)
γ (°)	85.402 (1)
<i>V</i> (Å ³)	1405.09 (6)
<i>D</i> _x (Mg m ⁻³)	1.499
Refinement	
<i>R</i> _p	0.0359
<i>R</i> _{wp}	0.0522
<i>R</i> _{exp}	0.0120
<i>R</i> _B	0.0371
<i>R</i> _F	0.0171

6. Powder diffraction characterization

An X-ray powder diffraction pattern of the title compound was registered using a Siemens D500 powder diffractometer (Cu $K\alpha$ radiation, Bragg–Brentano geometry, curved graphite monochromator on the counter arm, $4 < 2\theta < 60^\circ$, $D2\theta = 0.02^\circ$). A Rietveld refinement (Fig. 6) on the basis of the obtained pattern was carried out with *FullProf* and *WinPLOTR* (Rodriguez-Carvajal & Roisnel, 1998) using data of an external standard (NIST SRM1976) for the calculation of the instrumental profile function and the single-crystal data as the structure model for refinement. The main results of the Rietveld refinement are shown in Table 3. On the basis of the Rietveld refinement, the experimental powder X-ray diffraction pattern coincides with the theoretical one calculated from the X-ray single crystal study.

7. Synthesis and crystallization

4-[*(Benzylamino)carbonyl]-1-methylpyridinium iodide (57.7 g, 0.163 mol), silver bromide (33.77 g, 0.180 mol) and*

**Figure 6**

Final Rietveld plots for the title compound. Observed data points are indicated by red circles, the best-fit profile (black upper trace) and the difference pattern (blue lower trace) are shown as solid lines. The vertical green bars correspond to the Bragg reflections.

700 ml of water were loaded into a glass flask. The mixture was stirred for 72 h, and the resulting precipitate was filtered off. The solvent was evaporated under reduced pressure. To the precipitate were added 300 ml of acetonitrile and refluxed for 2 h. The reaction then was spontaneously cooled to a temperature of 303 K and the precipitate filtered off and rinsed on the filter with 50 ml of cooled acetonitrile. The product was dried at 313 K for 12 h. Yield: 14 g of 4-[(benzylamino)carbonyl]-1-methylpyridinium bromide (28%); colourless crystals.

8. Refinement

Crystal data, data collection and structure refinement details are summarized in Table 4. All of the hydrogen atoms were placed in calculated positions and treated as riding with C—H = 0.96 Å, $U_{\text{iso}}(\text{H}) = 1.5U_{\text{eq}}$ for methyl groups and with C_{ar}—H = 0.93 Å, C_{sp}^2 —H = 0.97 Å, $U_{\text{iso}}(\text{H}) = 1.2U_{\text{eq}}$ for all other hydrogen atoms.

Acknowledgements

The authors are grateful to Farmak JSC for support.

Funding information

Funding for this research was provided by: National Academy of Sciences of Ukraine (grant No. 0120U102660).

References

- Boltz, D., Peng, X., Muzzio, M., Dash, P., Thomas, P. G. & Margitich, V. (2018). *Antivir. Chem. Chemother.* **26**, 1–9.
 Buhtiarova, T. A., Danilenko, V. P., Homenko, V. S., Shatyrkina, T. V. & Yadlovsky, O. E. (2003). *Ukrainian Med. J.* **33**, 72–74.
 Dolomanov, O. V., Bourhis, L. J., Gildea, R. J., Howard, J. A. K. & Puschmann, H. (2009). *J. Appl. Cryst.* **42**, 339–341.
 Drebushchak, T. N., Kryukov, Y. A., Rogova, A. I. & Boldyreva, E. V. (2017). *Acta Cryst. E73*, 967–970.
 Frolov, A. F., Frolov, V. M., Buhtiarova, T. A. & Danilenko, V. P. (2004). *Ukrainian Med. J.* **39**, 69–74.
 Groom, C. R., Bruno, I. J., Lightfoot, M. P. & Ward, S. C. (2016). *Acta Cryst. B72*, 171–179.
 Macrae, C. F., Sovago, I., Cottrell, S. J., Galek, P. T. A., McCabe, P., Pidcock, E., Platings, M., Shields, G. P., Stevens, J. S., Towler, M. & Wood, P. A. (2020). *J. Appl. Cryst.* **53**, 226–235.

Table 4
Experimental details.

Crystal data	
Chemical formula	C ₁₄ H ₁₅ N ₂ O ⁺ ·Br ⁻ ·0.5H ₂ O
M _r	316.19
Crystal system, space group	Triclinic, <i>P</i> ī
Temperature (K)	293
a, b, c (Å)	5.8891 (4), 14.7565 (10), 17.8090 (11)
α, β, γ (°)	65.773 (6), 85.396 (6), 85.544 (6)
V (Å ³)	1405.08 (17)
Z	4
Radiation type	Mo <i>K</i> α
μ (mm ⁻¹)	2.92
Crystal size (mm)	0.30 × 0.15 × 0.10
Data collection	
Diffractometer	Xcalibur, Atlas
Absorption correction	Multi-scan (<i>CrysAlis PRO</i> ; Rigaku OD, 2021)
T _{min} , T _{max}	0.634, 1.000
No. of measured, independent and observed [I > 2σ(I)] reflections	14465, 4925, 3547
R _{int}	0.075
(sin θ/λ) _{max} (Å ⁻¹)	0.595
Refinement	
R[F ² > 2σ(F ²)], wR(F ²), S	0.060, 0.175, 1.06
No. of reflections	4925
No. of parameters	339
H-atom treatment	H-atom parameters constrained
Δρ _{max} , Δρ _{min} (e Å ⁻³)	1.12, -0.45

Computer programs: *CrysAlis PRO* (Rigaku OD, 2021), *SHELXT* (Sheldrick, 2015a), *SHELXL* (Sheldrick, 2015b), *Mercury* (Macrae *et al.*, 2020), *OLEX2* (Dolomanov *et al.*, 2009).

- Rigaku OD (2021). *CrysAlis PRO*. Rigaku Oxford Diffraction, Yarnton, England.
 Rodriguez-Carvajal, J. & Roisnel, T. (1998). *International Union of Crystallography Newsletter*, **20**, 35–36.
 Sheldrick, G. M. (2015a). *Acta Cryst. A71*, 3–8.
 Sheldrick, G. M. (2015b). *Acta Cryst. A71*, 3–8.
 Turner, M. J., McKinnon, J. J., Wolff, S. K., Grimwood, D. J., Spackman, P. R., Jayatilaka, D. & Spackman, M. A. (2017). *CrystalExplorer17*. University of Western Australia. <http://Hirshfeldsurface.net>.
 Velthuis, A. J. W., te Zubkova, T. G., Shaw, M., Mehle, A., Boltz, D., Gmeinwieser, N., Stammer, H., Milde, J., Müller, L. & Margitich, V. (2021). *Antimicrob. Agents Chemother.* **65**, e02605–20.
 Zefirov, Yu. V. (1997). *Kristallografiya*, **42**, 936–958.

supporting information

Acta Cryst. (2022). E78, 496–499 [https://doi.org/10.1107/S2056989022003784]

4-[(Benzylamino)carbonyl]-1-methylpyridinium bromide hemihydrate: X-ray diffraction study and Hirshfeld surface analysis

Vitalii V. Rudiuk, Anna M. Shaposhnik, Vyacheslav M. Baumer, Igor A. Levandovskiy and Svitlana V. Shishkina

Computing details

Data collection: *CrysAlis PRO* (Rigaku OD, 2021); cell refinement: *CrysAlis PRO* (Rigaku OD, 2021); data reduction: *CrysAlis PRO* (Rigaku OD, 2021); program(s) used to solve structure: *SHELXT* (Sheldrick, 2015a); program(s) used to refine structure: *SHELXL* (Sheldrick, 2015b); molecular graphics: *Mercury* (Macrae *et al.*, 2020); software used to prepare material for publication: *OLEX2* (Dolomanov *et al.*, 2009).

4-[(Benzylamino)carbonyl]-1-methylpyridinium bromide hemihydrate

Crystal data

$\text{C}_{14}\text{H}_{15}\text{N}_2\text{O}^+\cdot\text{Br}^-\cdot 0.5\text{H}_2\text{O}$	$Z = 4$
$M_r = 316.19$	$F(000) = 644$
Triclinic, $P\bar{1}$	$D_x = 1.495 \text{ Mg m}^{-3}$
$a = 5.8891 (4) \text{ \AA}$	$\text{Mo K}\alpha$ radiation, $\lambda = 0.71073 \text{ \AA}$
$b = 14.7565 (10) \text{ \AA}$	Cell parameters from 4991 reflections
$c = 17.8090 (11) \text{ \AA}$	$\theta = 3.6\text{--}25.4^\circ$
$\alpha = 65.773 (6)^\circ$	$\mu = 2.92 \text{ mm}^{-1}$
$\beta = 85.396 (6)^\circ$	$T = 293 \text{ K}$
$\gamma = 85.544 (6)^\circ$	Plate, colorless
$V = 1405.08 (17) \text{ \AA}^3$	$0.30 \times 0.15 \times 0.10 \text{ mm}$

Data collection

Xcalibur, Atlas	14465 measured reflections
diffractometer	4925 independent reflections
Radiation source: Enhance (Mo) X-ray Source	3547 reflections with $I > 2\sigma(I)$
Detector resolution: 10.3779 pixels mm ⁻¹	$R_{\text{int}} = 0.075$
ω scans	$\theta_{\text{max}} = 25.0^\circ, \theta_{\text{min}} = 3.4^\circ$
Absorption correction: multi-scan	$h = -6 \rightarrow 6$
(CrysAlisPro; Rigaku OD, 2021)	$k = -16 \rightarrow 17$
$T_{\text{min}} = 0.634, T_{\text{max}} = 1.000$	$l = -21 \rightarrow 20$

Refinement

Refinement on F^2	339 parameters
Least-squares matrix: full	0 restraints
$R[F^2 > 2\sigma(F^2)] = 0.060$	Hydrogen site location: mixed
$wR(F^2) = 0.175$	H-atom parameters constrained
$S = 1.06$	$w = 1/[\sigma^2(F_o^2) + (0.0802P)^2 + 0.8154P]$
4925 reflections	where $P = (F_o^2 + 2F_c^2)/3$

$(\Delta/\sigma)_{\max} = 0.001$
 $\Delta\rho_{\max} = 1.12 \text{ e \AA}^{-3}$

$\Delta\rho_{\min} = -0.45 \text{ e \AA}^{-3}$

Special details

Geometry. All esds (except the esd in the dihedral angle between two l.s. planes) are estimated using the full covariance matrix. The cell esds are taken into account individually in the estimation of esds in distances, angles and torsion angles; correlations between esds in cell parameters are only used when they are defined by crystal symmetry. An approximate (isotropic) treatment of cell esds is used for estimating esds involving l.s. planes.

Fractional atomic coordinates and isotropic or equivalent isotropic displacement parameters (\AA^2)

	<i>x</i>	<i>y</i>	<i>z</i>	$U_{\text{iso}}^*/U_{\text{eq}}$
Br1A	0.68503 (10)	1.06475 (4)	0.84634 (4)	0.0614 (2)
Br1B	0.37067 (11)	0.44764 (5)	0.67323 (4)	0.0621 (2)
O1A	0.3136 (7)	0.6956 (3)	0.9887 (2)	0.0611 (11)
N1A	0.9794 (7)	0.7007 (3)	1.1351 (2)	0.0438 (10)
N1B	0.6285 (7)	0.7967 (3)	0.3685 (3)	0.0496 (11)
N2A	0.3986 (7)	0.8566 (3)	0.9181 (3)	0.0493 (11)
H2A	0.486736	0.902420	0.913909	0.059*
O1B	-0.0865 (8)	0.8195 (3)	0.5244 (3)	0.0766 (14)
N2B	0.0287 (8)	0.6602 (4)	0.5982 (3)	0.0518 (11)
H2B	0.133971	0.614443	0.603968	0.062*
C9B	-0.1252 (8)	0.6264 (4)	0.7400 (3)	0.0413 (12)
C9A	0.2998 (8)	0.8874 (4)	0.7765 (3)	0.0432 (12)
C2A	0.9195 (9)	0.7968 (4)	1.0910 (3)	0.0473 (13)
H2AA	0.996826	0.846374	1.096125	0.057*
C10B	-0.2902 (9)	0.5848 (4)	0.8037 (3)	0.0505 (14)
H10B	-0.423087	0.563252	0.792737	0.061*
C4A	0.6308 (8)	0.7478 (4)	1.0305 (3)	0.0406 (12)
C6A	0.8719 (9)	0.6286 (4)	1.1285 (3)	0.0440 (12)
H6A	0.915307	0.562491	1.159801	0.053*
C7A	0.4317 (8)	0.7654 (4)	0.9765 (3)	0.0431 (12)
C14A	0.5157 (9)	0.8564 (4)	0.7586 (3)	0.0484 (13)
H14A	0.618478	0.829285	0.800112	0.058*
C3A	0.7436 (9)	0.8223 (4)	1.0381 (3)	0.0471 (13)
H3A	0.701404	0.888839	1.007835	0.057*
C8A	0.2168 (9)	0.8807 (4)	0.8609 (3)	0.0516 (14)
H8AA	0.141562	0.943815	0.855334	0.062*
H8AB	0.104777	0.830227	0.883854	0.062*
C4B	0.2677 (9)	0.7633 (4)	0.4813 (3)	0.0435 (12)
C6B	0.4700 (10)	0.8688 (4)	0.3605 (4)	0.0576 (15)
H6B	0.481705	0.930081	0.315903	0.069*
C13A	0.5825 (10)	0.8647 (4)	0.6799 (4)	0.0572 (15)
H13A	0.730428	0.845033	0.668565	0.069*
C5A	0.6988 (9)	0.6501 (4)	1.0763 (3)	0.0456 (12)
H5A	0.626632	0.598873	1.071699	0.055*
C8B	-0.1697 (9)	0.6367 (4)	0.6549 (3)	0.0517 (14)
H8BA	-0.226852	0.574898	0.658879	0.062*

H8BB	-0.287947	0.688592	0.632632	0.062*
C14B	0.0695 (9)	0.6561 (4)	0.7590 (3)	0.0495 (13)
H14B	0.182173	0.683315	0.717605	0.059*
C10A	0.1499 (9)	0.9266 (4)	0.7139 (3)	0.0509 (14)
H10A	0.003602	0.948655	0.724536	0.061*
C13B	0.1036 (10)	0.6469 (4)	0.8380 (3)	0.0560 (14)
H13B	0.236700	0.667865	0.849318	0.067*
C11B	-0.2587 (10)	0.5752 (5)	0.8820 (4)	0.0600 (16)
H11B	-0.370718	0.547599	0.923613	0.072*
C1A	1.1677 (9)	0.6740 (5)	1.1928 (3)	0.0537 (15)
H1AA	1.250770	0.732005	1.181669	0.080*
H1AB	1.268614	0.623796	1.185187	0.080*
H1AC	1.104851	0.649076	1.248552	0.080*
C12B	-0.0633 (10)	0.6060 (5)	0.8998 (4)	0.0591 (15)
H12B	-0.043285	0.599418	0.953119	0.071*
C7B	0.0549 (9)	0.7494 (4)	0.5377 (3)	0.0490 (13)
C2B	0.6158 (10)	0.7092 (4)	0.4317 (3)	0.0575 (15)
H2BA	0.729127	0.659726	0.436849	0.069*
C12A	0.4310 (11)	0.9020 (5)	0.6185 (4)	0.0653 (17)
H12A	0.473938	0.905876	0.565843	0.078*
C3B	0.4378 (10)	0.6904 (4)	0.4896 (3)	0.0540 (14)
H3B	0.431425	0.628916	0.534200	0.065*
C5B	0.2912 (10)	0.8543 (4)	0.4166 (3)	0.0560 (15)
H5B	0.184373	0.906179	0.411098	0.067*
C11A	0.2154 (11)	0.9334 (5)	0.6356 (4)	0.0658 (17)
H11A	0.112389	0.959471	0.594095	0.079*
C1B	0.8149 (11)	0.8123 (5)	0.3041 (4)	0.0697 (18)
H1BA	0.752677	0.819184	0.253735	0.105*
H1BB	0.922527	0.756296	0.321780	0.105*
H1BC	0.890242	0.871600	0.295088	0.105*
O1W	0.1099 (12)	0.5752 (7)	0.4262 (5)	0.132 (3)
H1WA	0.222090	0.534776	0.446576	0.198*
H1WB	0.054401	0.561287	0.389761	0.198*

Atomic displacement parameters (\AA^2)

	U^{11}	U^{22}	U^{33}	U^{12}	U^{13}	U^{23}
Br1A	0.0648 (4)	0.0476 (4)	0.0676 (4)	-0.0142 (3)	-0.0086 (3)	-0.0165 (3)
Br1B	0.0719 (4)	0.0510 (4)	0.0559 (4)	-0.0091 (3)	-0.0022 (3)	-0.0133 (3)
O1A	0.068 (3)	0.049 (2)	0.061 (2)	-0.0199 (19)	-0.0167 (19)	-0.0110 (19)
N1A	0.050 (2)	0.047 (3)	0.033 (2)	-0.0052 (19)	-0.0020 (17)	-0.015 (2)
N1B	0.056 (3)	0.052 (3)	0.041 (2)	-0.016 (2)	0.0023 (19)	-0.018 (2)
N2A	0.054 (3)	0.045 (3)	0.045 (2)	-0.0116 (19)	-0.0074 (19)	-0.011 (2)
O1B	0.069 (3)	0.059 (3)	0.075 (3)	0.002 (2)	0.018 (2)	-0.005 (2)
N2B	0.058 (3)	0.052 (3)	0.040 (2)	-0.003 (2)	0.0033 (19)	-0.015 (2)
C9B	0.044 (3)	0.038 (3)	0.039 (3)	-0.007 (2)	-0.002 (2)	-0.011 (2)
C9A	0.046 (3)	0.033 (3)	0.046 (3)	-0.007 (2)	-0.008 (2)	-0.009 (2)
C2A	0.062 (3)	0.036 (3)	0.043 (3)	-0.008 (2)	-0.009 (2)	-0.012 (2)

C10B	0.043 (3)	0.054 (4)	0.053 (3)	-0.015 (2)	0.007 (2)	-0.020 (3)
C4A	0.049 (3)	0.041 (3)	0.032 (3)	-0.007 (2)	0.001 (2)	-0.015 (2)
C6A	0.053 (3)	0.033 (3)	0.039 (3)	-0.003 (2)	-0.004 (2)	-0.008 (2)
C7A	0.049 (3)	0.045 (3)	0.036 (3)	-0.009 (2)	0.002 (2)	-0.016 (2)
C14A	0.048 (3)	0.041 (3)	0.052 (3)	-0.002 (2)	-0.011 (2)	-0.013 (2)
C3A	0.057 (3)	0.034 (3)	0.048 (3)	-0.006 (2)	-0.007 (2)	-0.013 (2)
C8A	0.045 (3)	0.051 (4)	0.052 (3)	0.001 (2)	-0.011 (2)	-0.013 (3)
C4B	0.054 (3)	0.043 (3)	0.033 (3)	-0.005 (2)	-0.005 (2)	-0.015 (2)
C6B	0.064 (4)	0.040 (3)	0.054 (3)	-0.007 (3)	0.003 (3)	-0.005 (3)
C13A	0.058 (3)	0.051 (4)	0.062 (4)	0.000 (3)	-0.004 (3)	-0.023 (3)
C5A	0.057 (3)	0.037 (3)	0.043 (3)	-0.012 (2)	0.003 (2)	-0.016 (2)
C8B	0.058 (3)	0.049 (3)	0.043 (3)	-0.009 (2)	0.000 (2)	-0.012 (3)
C14B	0.050 (3)	0.043 (3)	0.048 (3)	-0.010 (2)	0.005 (2)	-0.012 (3)
C10A	0.043 (3)	0.050 (3)	0.052 (3)	-0.001 (2)	-0.013 (2)	-0.011 (3)
C13B	0.060 (3)	0.058 (4)	0.055 (4)	-0.009 (3)	-0.007 (3)	-0.025 (3)
C11B	0.064 (4)	0.063 (4)	0.050 (3)	-0.019 (3)	0.018 (3)	-0.021 (3)
C1A	0.047 (3)	0.060 (4)	0.049 (3)	0.000 (3)	-0.014 (2)	-0.016 (3)
C12B	0.072 (4)	0.062 (4)	0.046 (3)	-0.004 (3)	-0.002 (3)	-0.025 (3)
C7B	0.051 (3)	0.051 (4)	0.039 (3)	-0.001 (3)	-0.003 (2)	-0.013 (3)
C2B	0.065 (4)	0.045 (4)	0.056 (4)	0.000 (3)	0.002 (3)	-0.015 (3)
C12A	0.079 (4)	0.061 (4)	0.061 (4)	-0.012 (3)	0.000 (3)	-0.029 (3)
C3B	0.063 (3)	0.045 (3)	0.042 (3)	-0.003 (3)	0.004 (2)	-0.007 (3)
C5B	0.058 (3)	0.045 (3)	0.054 (3)	0.001 (3)	0.004 (3)	-0.011 (3)
C11A	0.068 (4)	0.063 (4)	0.062 (4)	0.002 (3)	-0.022 (3)	-0.019 (3)
C1B	0.067 (4)	0.072 (5)	0.062 (4)	-0.012 (3)	0.019 (3)	-0.021 (3)
O1W	0.103 (5)	0.189 (8)	0.132 (6)	0.013 (5)	-0.021 (4)	-0.095 (6)

Geometric parameters (\AA , $^\circ$)

O1A—C7A	1.223 (6)	C4B—C5B	1.373 (7)
N1A—C6A	1.330 (7)	C4B—C3B	1.382 (7)
N1A—C2A	1.343 (6)	C4B—C7B	1.514 (7)
N1A—C1A	1.491 (7)	C6B—C5B	1.357 (8)
N1B—C2B	1.323 (7)	C6B—H6B	0.9300
N1B—C6B	1.329 (7)	C13A—C12A	1.372 (9)
N1B—C1B	1.480 (7)	C13A—H13A	0.9300
N2A—C7A	1.332 (6)	C5A—H5A	0.9300
N2A—C8A	1.459 (7)	C8B—H8BA	0.9700
N2A—H2A	0.8600	C8B—H8BB	0.9700
O1B—C7B	1.231 (6)	C14B—C13B	1.386 (8)
N2B—C7B	1.326 (7)	C14B—H14B	0.9300
N2B—C8B	1.446 (7)	C10A—C11A	1.382 (8)
N2B—H2B	0.8600	C10A—H10A	0.9300
C9B—C14B	1.373 (7)	C13B—C12B	1.384 (8)
C9B—C10B	1.397 (7)	C13B—H13B	0.9300
C9B—C8B	1.502 (7)	C11B—C12B	1.375 (9)
C9A—C14A	1.376 (7)	C11B—H11B	0.9300
C9A—C10A	1.381 (7)	C1A—H1AA	0.9600

C9A—C8A	1.507 (8)	C1A—H1AB	0.9600
C2A—C3A	1.381 (8)	C1A—H1AC	0.9600
C2A—H2AA	0.9300	C12B—H12B	0.9300
C10B—C11B	1.370 (8)	C2B—C3B	1.370 (8)
C10B—H10B	0.9300	C2B—H2BA	0.9300
C4A—C5A	1.379 (7)	C12A—C11A	1.372 (9)
C4A—C3A	1.385 (7)	C12A—H12A	0.9300
C4A—C7A	1.515 (7)	C3B—H3B	0.9300
C6A—C5A	1.365 (8)	C5B—H5B	0.9300
C6A—H6A	0.9300	C11A—H11A	0.9300
C14A—C13A	1.383 (8)	C1B—H1BA	0.9600
C14A—H14A	0.9300	C1B—H1BB	0.9600
C3A—H3A	0.9300	C1B—H1BC	0.9600
C8A—H8AA	0.9700	O1W—H1WA	0.8506
C8A—H8AB	0.9700	O1W—H1WB	0.8502
C6A—N1A—C2A	120.9 (4)	C6A—C5A—H5A	120.0
C6A—N1A—C1A	119.3 (4)	C4A—C5A—H5A	120.0
C2A—N1A—C1A	119.9 (5)	N2B—C8B—C9B	114.0 (5)
C2B—N1B—C6B	120.5 (5)	N2B—C8B—H8BA	108.8
C2B—N1B—C1B	119.4 (5)	C9B—C8B—H8BA	108.8
C6B—N1B—C1B	120.0 (5)	N2B—C8B—H8BB	108.8
C7A—N2A—C8A	121.7 (5)	C9B—C8B—H8BB	108.8
C7A—N2A—H2A	119.1	H8BA—C8B—H8BB	107.6
C8A—N2A—H2A	119.1	C9B—C14B—C13B	122.1 (5)
C7B—N2B—C8B	122.7 (5)	C9B—C14B—H14B	119.0
C7B—N2B—H2B	118.6	C13B—C14B—H14B	119.0
C8B—N2B—H2B	118.6	C9A—C10A—C11A	120.6 (5)
C14B—C9B—C10B	117.7 (5)	C9A—C10A—H10A	119.7
C14B—C9B—C8B	123.6 (4)	C11A—C10A—H10A	119.7
C10B—C9B—C8B	118.7 (5)	C12B—C13B—C14B	119.1 (6)
C14A—C9A—C10A	118.3 (5)	C12B—C13B—H13B	120.5
C14A—C9A—C8A	123.7 (4)	C14B—C13B—H13B	120.5
C10A—C9A—C8A	118.0 (5)	C10B—C11B—C12B	120.7 (5)
N1A—C2A—C3A	120.4 (5)	C10B—C11B—H11B	119.7
N1A—C2A—H2AA	119.8	C12B—C11B—H11B	119.7
C3A—C2A—H2AA	119.8	N1A—C1A—H1AA	109.5
C11B—C10B—C9B	120.8 (5)	N1A—C1A—H1AB	109.5
C11B—C10B—H10B	119.6	H1AA—C1A—H1AB	109.5
C9B—C10B—H10B	119.6	N1A—C1A—H1AC	109.5
C5A—C4A—C3A	118.6 (5)	H1AA—C1A—H1AC	109.5
C5A—C4A—C7A	116.8 (5)	H1AB—C1A—H1AC	109.5
C3A—C4A—C7A	124.7 (5)	C11B—C12B—C13B	119.7 (6)
N1A—C6A—C5A	120.9 (5)	C11B—C12B—H12B	120.2
N1A—C6A—H6A	119.5	C13B—C12B—H12B	120.2
C5A—C6A—H6A	119.5	O1B—C7B—N2B	123.4 (5)
O1A—C7A—N2A	124.3 (5)	O1B—C7B—C4B	119.2 (5)
O1A—C7A—C4A	118.4 (5)	N2B—C7B—C4B	117.4 (5)

N2A—C7A—C4A	117.2 (5)	N1B—C2B—C3B	120.8 (5)
C9A—C14A—C13A	121.1 (5)	N1B—C2B—H2BA	119.6
C9A—C14A—H14A	119.4	C3B—C2B—H2BA	119.6
C13A—C14A—H14A	119.4	C13A—C12A—C11A	119.2 (6)
C2A—C3A—C4A	119.3 (5)	C13A—C12A—H12A	120.4
C2A—C3A—H3A	120.4	C11A—C12A—H12A	120.4
C4A—C3A—H3A	120.4	C2B—C3B—C4B	119.6 (5)
N2A—C8A—C9A	113.5 (4)	C2B—C3B—H3B	120.2
N2A—C8A—H8AA	108.9	C4B—C3B—H3B	120.2
C9A—C8A—H8AA	108.9	C6B—C5B—C4B	120.2 (5)
N2A—C8A—H8AB	108.9	C6B—C5B—H5B	119.9
C9A—C8A—H8AB	108.9	C4B—C5B—H5B	119.9
H8AA—C8A—H8AB	107.7	C12A—C11A—C10A	120.6 (5)
C5B—C4B—C3B	117.8 (5)	C12A—C11A—H11A	119.7
C5B—C4B—C7B	117.6 (5)	C10A—C11A—H11A	119.7
C3B—C4B—C7B	124.6 (5)	N1B—C1B—H1BA	109.5
N1B—C6B—C5B	121.0 (5)	N1B—C1B—H1BB	109.5
N1B—C6B—H6B	119.5	H1BA—C1B—H1BB	109.5
C5B—C6B—H6B	119.5	N1B—C1B—H1BC	109.5
C12A—C13A—C14A	120.2 (6)	H1BA—C1B—H1BC	109.5
C12A—C13A—H13A	119.9	H1BB—C1B—H1BC	109.5
C14A—C13A—H13A	119.9	H1WA—O1W—H1WB	109.4
C6A—C5A—C4A	120.0 (5)		
C6A—N1A—C2A—C3A	0.3 (8)	C14B—C9B—C8B—N2B	12.8 (8)
C1A—N1A—C2A—C3A	-179.3 (5)	C10B—C9B—C8B—N2B	-167.4 (5)
C14B—C9B—C10B—C11B	0.7 (8)	C10B—C9B—C14B—C13B	-0.7 (8)
C8B—C9B—C10B—C11B	-179.0 (6)	C8B—C9B—C14B—C13B	179.0 (5)
C2A—N1A—C6A—C5A	0.4 (8)	C14A—C9A—C10A—C11A	0.6 (8)
C1A—N1A—C6A—C5A	-180.0 (5)	C8A—C9A—C10A—C11A	-179.1 (6)
C8A—N2A—C7A—O1A	-1.5 (8)	C9B—C14B—C13B—C12B	0.3 (9)
C8A—N2A—C7A—C4A	177.9 (5)	C9B—C10B—C11B—C12B	-0.3 (10)
C5A—C4A—C7A—O1A	15.0 (7)	C10B—C11B—C12B—C13B	-0.1 (10)
C3A—C4A—C7A—O1A	-163.5 (5)	C14B—C13B—C12B—C11B	0.1 (9)
C5A—C4A—C7A—N2A	-164.4 (5)	C8B—N2B—C7B—O1B	-0.2 (9)
C3A—C4A—C7A—N2A	17.1 (7)	C8B—N2B—C7B—C4B	-178.4 (5)
C10A—C9A—C14A—C13A	0.5 (8)	C5B—C4B—C7B—O1B	-0.9 (8)
C8A—C9A—C14A—C13A	-179.8 (6)	C3B—C4B—C7B—O1B	-179.7 (6)
N1A—C2A—C3A—C4A	-0.5 (8)	C5B—C4B—C7B—N2B	177.4 (5)
C5A—C4A—C3A—C2A	-0.1 (8)	C3B—C4B—C7B—N2B	-1.4 (9)
C7A—C4A—C3A—C2A	178.4 (5)	C6B—N1B—C2B—C3B	0.9 (9)
C7A—N2A—C8A—C9A	-102.6 (6)	C1B—N1B—C2B—C3B	-176.0 (6)
C14A—C9A—C8A—N2A	11.4 (8)	C14A—C13A—C12A—C11A	1.9 (10)
C10A—C9A—C8A—N2A	-168.9 (5)	N1B—C2B—C3B—C4B	0.9 (10)
C2B—N1B—C6B—C5B	-0.3 (9)	C5B—C4B—C3B—C2B	-3.1 (9)
C1B—N1B—C6B—C5B	176.6 (6)	C7B—C4B—C3B—C2B	175.6 (6)
C9A—C14A—C13A—C12A	-1.8 (9)	N1B—C6B—C5B—C4B	-2.0 (10)
N1A—C6A—C5A—C4A	-1.0 (8)	C3B—C4B—C5B—C6B	3.7 (9)

C3A—C4A—C5A—C6A	0.8 (8)	C7B—C4B—C5B—C6B	-175.1 (6)
C7A—C4A—C5A—C6A	-177.8 (5)	C13A—C12A—C11A—C10A	-0.8 (10)
C7B—N2B—C8B—C9B	-107.0 (6)	C9A—C10A—C11A—C12A	-0.5 (10)

*Hydrogen-bond geometry (\AA , $^\circ$)*Cg*A* and Cg*B* are the centroids of the C9*A*—C14*A* and C9*B*—C14*B* rings, respectively.

D—H··· <i>A</i>	D—H	H··· <i>A</i>	D··· <i>A</i>	D—H··· <i>A</i>
N2 <i>A</i> —H2 <i>A</i> ···Br1 <i>A</i>	0.86	2.53	3.339 (5)	158
C3 <i>A</i> —H3 <i>A</i> ···Br1 <i>A</i>	0.93	2.98	3.814 (5)	150
C2 <i>A</i> —H2 <i>AA</i> ···Br1 <i>A</i> ⁱ	0.93	2.84	3.725 (6)	159
C1 <i>A</i> —H1 <i>AA</i> ···Br1 <i>A</i> ⁱ	0.96	2.88	3.784 (6)	157
C6 <i>A</i> —H6 <i>A</i> ···Cg <i>B</i> ⁱⁱ	0.93	2.65	3.510 (7)	154
N2 <i>B</i> —H2 <i>B</i> ···Br1 <i>B</i>	0.86	2.60	3.419 (5)	159
C3 <i>B</i> —H3 <i>B</i> ···Br1 <i>B</i>	0.93	2.83	3.753 (5)	175
C6 <i>B</i> —H6 <i>B</i> ···Cg <i>A</i> ⁱⁱⁱ	0.93	2.71	3.400 (7)	132
O1 <i>W</i> —H1 <i>WA</i> ···Br1 <i>B</i> ^{iv}	0.85	3.03	3.473 (7)	115
C1 <i>A</i> —H1 <i>AC</i> ···O1 <i>W</i> ^v	0.96	2.89	3.794 (10)	157

Symmetry codes: (i) $-x+2, -y+2, -z+2$; (ii) $-x+1, -y+1, -z+2$; (iii) $-x+1, -y+2, -z+1$; (iv) $-x+1, -y+1, -z+1$; (v) $x+1, y, z+1$.